The Journal of Physical Chemistry B

 VOLUME 102, NUMBER 20, MAY 14, 1998

FEATURE ARTICLE

Investigations of the Structure and Hydrogen Bonding of Water Molecules at Liquid Surfaces by Vibrational Sum Frequency Spectroscopy

D. E. Gragson† and G. L. Richmond*

Department of Chemistry, University of Oregon, Eugene, Oregon 97403

Received: December 30, 1997; In Final Form: March 12, 1998

The structure and hydrogen bonding of water molecules provides this unique solvent with properties essential to many physical, chemical, and biological processes. The intermolecular hydrogen bonding between water molecules in the bulk medium is disrupted at the surface, imparting the surface with unique structural and thermodynamic properties. We provide an overview of a range of experimental studies from this laboratory in which the structure, orientation, and hydrogen bonding of interfacial water molecules at liquid interfaces are directly probed by resonant vibrational sum frequency spectroscopy. The studies provide insight into the difference in water structure and hydrogen bonding at an air/water interface relative to the interface between two bulk immiscible liquids, namely the CCl_4/H_2O interface. Also described are studies aimed at understanding how the presence of a charged alkyl surfactant alters the structure of water at these two interfaces. In both cases field-induced alignment of water molecules in the double layer region is prevalent. This induced alignment has been examined under a variety of experimental conditions. A series of isotopic dilution studies conducted for the first time at liquid surfaces are also described. In these studies the intermolecular and intramolecular coupling of vibrational modes in the water molecules are diminished. The results of these and above-mentioned studies provide valuable information for those interested in developing theoretical descriptions of water at surfaces and interfaces.

A. Introduction

Water is the foundation for everything that lives. Over the centuries, scientists have been interested in the relationship between the molecular structure of water and its unique properties. These unique properties are central to the function of many chemical, physical, and biological processes.[1] Many of these processes occur at water or aqueous surfaces where the strong hydrogen bonding between water molecules leads to distinctly different thermodynamic properties, such as a relatively high surface tension, a relatively low vapor pressure, and a high heat of vaporization. Although we have a general idea of how the molecular structure and hydrogen bonding of water molecules can lead to such interesting surface properties for water, it is only with recent advances in molecular dynamics calculations and experimental methods that we are beginning to understand how the molecular structure of surface water is perturbed by an adjacent immiscible liquid phase or by the presence of surfactants, ions, and adsorbates.

Ongoing experiments in this laboratory over the past few years have focused on measuring the molecular structure and bonding interactions at aqueous surfaces and interfaces.[2−5] The experiments are driven by a desire to understand the correlation between the macroscopic properties of the surface and the microscopic properties such as molecular structure, hydrogen bonding, and intermolecular coupling of surface water mol-

† Current address: Department of Chemistry, Harvey Mudd College, 301 E. Twelfth St., Claremont, CA 91711.

S1089-5647(98)00601-4 CCC: $15.00
Published on Web 04/17/1998

TABLE 1: Frequencies and Designations for SF-Active Modes Observed under SSP Polarization Conditions in VSFG Spectra from Various Interfaces

designation	assignment	frequency (cm^{-1})	reference
NH_3^+-FR	NH_3^+ Fermi resonance	2700	this study
CH_2-SS	CH_2 symmetric stretch	2850	2, 3, 33
CH_3-SS	CH_3 symmetric stretch	2875	2, 3, 33
CH_2-FR	CH_2 Fermi resonance	2900	3, 12
CH_2-AS	CH_2 asymmetric stretch	2925	2, 3, 33
CH_3-FR	CH_3 Fermi resonance	2935	2, 3, 33
OH-SS-S	ice-like, high H-bond order, O−H stretch	3200	4, 5
OH-SS-A	water-like, low H-bond order, O−H stretch	3450	4, 5
HOD,OH-S	inter and intramolecularly uncoupled O−H stretch	3300−3500	this study
free-OH	non-hydrogen bonded O−H stretch	3680	5, 15

ecules. This article provides an overview of a series of studies from this laboratory that provide a wealth of information about water at the air/water and oil/water interface. The results show the very different nature of interfacial water at the interface between two immiscible liquids relative to the air/water interface and how interfacial water structure and hydrogen bonding are affected by charged surfactants and the accompanying surface potential. It is hoped that the results of these studies will stimulate further the discussion of the properties of aqueous liquid surfaces and provide new information for theoretical efforts in this area.

To probe these surface properties, we have employed a combination of the second-order nonlinear optical method, vibrational sum frequency spectroscopy (VSFS), and interfacial tension measurements. VSFS is a very powerful technique for studying surfaces for a variety of reasons, the most notable being (1) its inherent surface sensitivity arising from the second-order nature of this nonlinear optical technique, (2) its molecular specificity arising from the resonant nature of the response, and (3) its wide applicability to a range of surfaces and interfaces. As these studies demonstrate, the nonlinear vibrational spectroscopy of these interfaces is rich with information that we and others have only begun to unravel.

B. Vibrational Sum Frequency Response from Liquid Surfaces

Vibrational sum frequency spectroscopy (VSFS) is a nonlinear optical technique that has been extensively used in the study of surfaces and interfaces.[6−11] VSFS is a second-order process, and therefore under the dipole approximation it is forbidden in media that possess inversion symmetry. At the interface between two centrosymmetric media there is no inversion center, and thus VSFS is allowed in this region. The asymmetric nature of interfaces allows one to specifically probe the interfacial region using VSFS. Typically, one combines a visible laser beam and a tunable infrared laser beam at the interface with the energy range of the tunable IR laser overlapping with the energies of vibrational modes of molecules present at the interface. By scanning the energy of the IR laser and monitoring the generated sum frequency signal, one obtains a vibrational spectrum of the interfacial molecules. The VSFS intensity is proportional to the square of the surface nonlinear susceptibility $\chi_s^{(2)}(\omega_{sfg}=\omega_{vis}+\omega_{ir})$ as

$$I_{sfg} \propto |P_{sfg}|^2 \propto |\chi_{NR}^{(2)} + \sum_v |\chi_{R_v}(2)|e^{i\gamma_v}|^2 I_{vis} I_{ir} \qquad (1)$$

where P_{sfg} is the nonlinear polarization at ω_{sfg}, χ_{NR} and χ_{R_v} are the nonresonant and resonant parts of $\chi_s^{(2)}$, γ_v is the relative phase of the vth vibrational mode, and I_{vis} and I_{ir} are the visible and IR intensities. Since the susceptibility is in general complex, the resonant terms in the summation are associated with a relative phase γ_v which is used to account for any interference between two modes that overlap in energy. $\chi_{R_v}^{(2)}$ is also proportional to the number density of molecules, N, and the orientationally averaged molecular hyperpolarizability, β_v, as follows:

$$\chi_{R_v}^{(2)} = (N/\epsilon_0)\langle\beta_v\rangle \qquad (2)$$

Thus, the square root of the measured SF intensity is proportional to the number density of molecules at the surface or interface. The molecular hyperpolarizability, β_v, is enhanced when the frequency of the IR field is resonant with a SF-active vibrational mode from a molecule at the surface or interface. This enhancement in β_v leads to an enhancement in the nonlinear susceptibility $\chi_{R_v}^{(2)}$ which can be expressed as

$$\chi_{R_v}^{(2)} \propto \frac{A_v}{\omega_v - \omega_{ir} - i\Gamma_v} \qquad (3)$$

where A_v is the intensity of the vth mode and is proportional to the product of the Raman and the IR transition moments, ω_v is the resonant frequency, and Γ_v is the line width of the transition. Since the intensity term, A_v, is proportional to both the IR and Raman transition moments, only vibrational modes that are both IR- and Raman-active will be SF-active. Thus, molecules or vibrational modes that possess an inversion center will not be SF-active.

In general, the surface susceptibility $\chi_s^{(2)}$ is a 27-element tensor; however, it can often be reduced to several nonvanishing elements by invoking symmetry constraints. Liquid surfaces and interfaces as well as monolayers on liquid surfaces are isotropic in the plane of the surface. The symmetry constraints for an in-plane isotropic surface reduces $\chi_s^{(2)}$ to the following four independent nonzero elements

$$\chi_{zzz}^{(2)}, \chi_{xxz}^{(2)} = \chi_{yyz}^{(2)}, \chi_{xzx}^{(2)} = \chi_{yzy}^{(2)}, \chi_{zxx}^{(2)} = \chi_{zyy}^{(2)} \qquad (4)$$

where z is defined to be the direction normal to the surface. These four independent elements contribute to the VSFS signal under the four different polarization conditions SSP, SPS, PSS, and PPP where the polarizations are listed in the order of decreasing frequency (sf, vis, ir). Which vibrational modes are present under a certain polarization condition depends on the polarization of the IR field and the direction of the IR and Raman transition moments. The SSP polarization condition accesses vibrational modes with transition moments that have components perpendicular to the surface plane whereas the SPS and PSS polarization conditions access modes that have transition moments with components parallel to the surface plane (Table 1). The intensity under PPP polarization conditions contains contributions from all of the tensor elements; thus, vibrational modes with components both perpendicular and

parallel to the surface plane will be present in the PPP polarized VSFS spectra. For the systems in this study, the most valuable vibrational modes of the interfacial water molecules all possess transition moments with components out of the plane of the surface. Consequently, we confine our discussion to in this paper to the SSP polarization condition. However, verification of the peak assignments has been made from spectra using all of the polarization combinations.

Many of the systems to be described here examine the structure of H_2O at an interface in the presence of a charged surfactant. At an interface where charged surfactant is adsorbed a significant surface charge exists which produces a large electrostatic field E_0. This electrostatic field can make an additional contribution to the nonlinear polarization induced at the interface by the optical fields E_{vis} and E_{ir} through a third-order polarization term $\chi^{(3)}$ as follows:

$$P_{sfg} = \chi^{(2)}:E_{vis}E_{ir} + \chi^{(3)}:E_{vis}E_{ir}E_0 \quad (5)$$

The second term in eq 5 is the third-order polarization term, $P^{(3)}_{sfg}$, and contains the electrostatic field dependence of the nonlinear polarization induced at the interface. Both $\chi^{(3)}$ and $\chi^{(2)}$ have resonant and nonresonant portions as described above, and in fact, the overall SF response can be represented by an effective surface susceptibility which is a combination of $\chi^{(3)}$ and $\chi^{(2)}$. In the absence of a large electrostatic field, one would expect the interfacial water molecules to be randomly oriented after a few water layers and thus to not contribute to the nonlinear polarization. The presence of a large electrostatic field aligns the interfacial water molecules beyond the first few water layers and thus removes the centrosymmetry over this region, allowing more water molecules to contribute to the nonlinear polarization. The depth of the asymmetric region is on the order of the Debye length, or 3 nm at an ionic strength of 10 mM and 10 nm at an ionic strength of 1.0 mM corresponding to approximately 10 to 30 water layers, respectively. Previous studies have shown that this alignment of the interfacial water molecules is manifested in the VSFS spectra as a large enhancement in the SF response in the OH stretching spectral region.[5,8] This electrostatic field-dependent enhancement results from a combination of an increased number of water molecules interacting with the optical fields and an alignment of the transition dipole moments of the OH modes with the polarization vector of the IR light.

Nonresonant second harmonic studies at the air/water interface with an insoluble charged surfactant present have shown[12] that the SHG intensity is dependent on the interfacial potential which, in turn, is dependent on the surface charge density and the ionic strength of the surfactant solution. For VSFS the relationship between the nonlinear polarization and the interfacial potential can be obtained by integrating $P^{(3)}_{sfg}$ over the region where the electrostatic field, E_0, is present. Assuming $\chi^{(3)}$ is constant over the interfacial region and using the relationship between the electrostatic field $E(z)$ and the interfacial potential $\Phi(z)$, one obtains

$$P_{sfg} = \chi^{(2)}E_{vis}E_{ir} + \chi^{(3)}E_{vis}E_{ir}\Phi(0)$$
$$= [\chi^{(2)} + \chi^{(3)}\Phi(0)]E_{vis}E_{ir} \quad (6)$$

where $\Phi(0)$ is the potential at the interface where $z = 0$. Equation 6 demonstrates the linear dependence of the nonlinear polarization on the interfacial potential.

In the work presented here we monitor the structure and hydrogen bonding of interfacial water molecules as the interfacial potential is varied. The Gouy−Chapman model has been shown to accurately characterize the interfacial potential as a function of surface charge density and ionic strength.[12,13] Using this model, the interfacial potential is expressed as

$$\Phi(0) = \frac{2kT}{ze}\sinh^{-1}\left[\sigma\left(\frac{\pi}{2\epsilon kTI}\right)^{1/2}\right] \quad (7)$$

where σ is the surface charge density, z is the sign of the charged surfactant molecule, ϵ is the permittivity of free space, and I is the ionic strength of the bulk solution. We obtain the surface charge density from surface tension measurements employing a Wilhelmy balance. Within the confines of the Gouy−Chapman model, the depth of the interfacial region, called the double-layer region or the Debye−Hückel screening length, over which the electrostatic field is present can be expressed as

$$\frac{1}{\kappa} = \left(\frac{1000DRT}{8\pi N^2\epsilon^2 I}\right)^{1/2} = 0.3/I^{1/2}\ (\text{nm}) \quad (8)$$

where D is the dielectric constant and I is the ionic strength of the bulk solution in mol/L. Increasing the bulk surfactant concentration increases the surface concentration and the surface charge density, thereby resulting in an increased interfacial potential. Varying the ionic strength of the solution has a twofold effect on the electrostatic field created by the soluble charged surfactants used in this study. One effect is a change in the Debye−Hückel screening length, eq 8, brought about by a change in the number of ions present at the interface. For example, as the ionic strength increases, the number of ions at the interface increases and the surface charge is screened in a smaller distance. The smaller Debye−Hückel screening length means that fewer interfacial water molecules interact with the electrostatic electric field which in turn produces a smaller nonlinear polarization. The other effect is a reduction in the interfacial potential, eq 7, that accompanies increasing ionic strength. Also pertinent to consider is that the surface concentration of soluble surfactants and thus the surface charge density are dependent on the ionic strength of the solution. For a bulk SDS concentration of 4.00 mM the surface concentration increases by 10−15% over the range of ionic strengths studied here with most of the increase achieved before an ionic strength of 0.05 M.

C. Experimental Considerations

The laser system employed for the vibrational SFG studies has been described in detail elsewhere.[14,15] Briefly, it consists of a titanium:sapphire regenerative amplifier which pumps a two-stage optical parametric amplifier seeded with a small portion of white light continuum generated in ethylene glycol. The system produces IR pulses tunable from 2.4 to 4.0 μm at a repetition rate of 1 kHz. The energy of the pulses over this range is approximately 8 μJ with a bandwidth of 18 cm^{-1} and a pulse duration of 1.9 ps. The IR pulses are combined at the interface with approximately 150 μJ of 800 nm light from the Ti:sapphire regenerative amplifier. All spectra presented were obtained under S_{sfg}, S_{vis}, P_{ir} polarization conditions which picks out the vibrational modes with components of the transition dipole moment perpendicular to the plane of the interface. Spectra from the air/water interface were obtained in an external reflection geometry with the 800 nm and IR beams directed onto the interface in a copropagating arrangement at angles of 56° and 68° from the surface normal, respectively. The beam

diameters of the tunable IR and 800 nm laser beams used in the air/water studies were approximately 300 and 800 μm, respectively. Spectra from the CCl_4/water interface were obtained in a total internal reflection geometry with the 800 nm and tunable IR beams coincident on the interface from the CCl_4 side at the critical angle for each wavelength (66.5° and 73.2°, respectively). The beam diameter of the tunable IR and 800 nm laser beams for the CCl_4/water studies was approximately 300 μm and 4 mm, respectively. Generation of fluorescence and continuum in the CCl_4 by the 800 nm beam necessitated the beam expansion (as compared to the air/water studies) to 4 mm. Previous studies[3,7] have shown that operating in a total internal reflection geometry produces an enhancement of several orders of magnitude in the generated nonlinear polarization. For both geometries the generated sum frequency light is detected in reflection with a PMT after filtering. Individual spectra were collected with gated electronics and a computer while the IR frequency was scanned from 2750 to 3700 cm^{-1}. The laser system limits our ability to obtain spectra in the 3600−4000 cm^{-1} region, and thus we have not included this region in our discussion.[15] Each scan was obtained with an increment of 4 cm^{-1} and an average of 300 laser shots per increment, and each spectrum presented is an average of at least two scans. We obtain peak intensities, bandwidths, areas, and positions from least-squares fits to the spectral data using eqs 1 and 3.

Both 18 MΩ water from a Nanopure filtration system and HPLC grade water from Mallinckrodt were used with no detectable difference in the VSFS spectra or in surface tension measurements performed with a Wilhelmy balance. Carbon tetrachloride (99.9+% HPLC grade) from Sigma-Aldrich was used as received. Sodium dodecyl sulfate (98% atom d-25) from Cambridge isotope laboratories was used as received. The bulk concentration of SDS in the aqueous phase was increased by additions of a stock solution followed by gentle stirring. After each addition 20−30 min was allowed for the interfacial adsorption of SDS to occur before a spectral scan was obtained. From surface tension measurements performed with a Wilhelmy balance and the Gibbs equation for adsorption we calculate the surface density of SDS. The surface density measurements are consistent with literature measurements conducted at the same ionic strength.[16,17] The surface potential is calculated using Gouy−Chapman theory and the assumption that each SDS molecule is charged. Absorption of the tunable IR beam in the OH stretching region by the CCl_4 was determined to be negligible with FTIR and by monitoring the IR energy from the laser system after the beam had traversed a 1 cm path length of CCl_4. All glassware and experimental apparatus that came into contact with the aqueous or organic phases were soaked in concentrated sulfuric acid containing No-Chromix for at least 3 h and then were thoroughly rinsed with 18 MΩ water.

D. Hydrogen Bonding and Structure at Neat Water Surfaces

At the water surface, the hydrogen bonding in bulk water is disrupted by the asymmetry created by the surface or interfacial region. This altered hydrogen bonding of water molecules at this surface has long been assumed responsible for the unique properties of aqueous surfaces including a surface tension significantly higher than predicted from homologous molecules. Shen and co-workers[8,18] demonstrated in previous VSFG studies the qualitative difference between the structure of water at the air/water interface relative to what is found in IR and Raman studies of bulk water. In this laboratory it has been shown that the water structure at the air/water interface is considerably different than what is found at the CCl_4/H_2O interface.[19] The studies described in this section summarize the results of these studies with a particular focus on the differences between hydrogen bonding of interfacial water molecules at the air/water and CCl_4/water interfaces.

The vibrational spectroscopy of bulk water and ice is complex and has been studied extensively by both IR and Raman spectroscopy. The complexity arises due to coupling across hydrogen bonds and energetic coupling of many normal modes, making assignment of normal modes of each peak difficult. Nevertheless, previous IR and Raman studies of bulk water[20−22] have been able to provide assignments to many of these modes which have furthered our understanding of the vibrational structure that we observe at the air/water and CCl_4/water interfaces by VSFS.

The VSFS water surface studies described herein have been restricted to the 2800−4000 cm^{-1} region corresponding to the OH stretch modes of water. In this region several spectral features observed for surface water[8,19] by VSFS are similar to what is been observed in the previous bulk water studies conducted with IR and Raman spectroscopy.[20−22] Two OH peaks characteristic of hydrogen-bonded water molecules appear near 3200 $^{-}$ and 3400 cm^{-1}. Based largely on spectral assignments made in these previous IR and Raman studies, the first peak at 3200 cm^{-1} is attributed to the in-phase vibrations of the coupled OH stretching modes of tetrahedrally coordinated water molecules and is designated as OH-SS-S here. This peak has been assumed to represent a high degree of hydrogen bond ordering and an ice-like structure in the molecular arrangement of the water molecules.[8,20,21,23] We refer to this peak as the OH-SS-S peak, indicative of the nature of the local symmetric hydrogen-bonding environment. The second peak occurs at approximately 3400 cm^{-1}. Two different modes have been suggested for this peak, both representing a somewhat lower degree of hydrogen-bonding structure. The first assignment is the coupled OH stretch from water molecules that are asymmetrically hydrogen bonded or in a more random and water-like molecular arrangement.[20] Other authors[24] have attributed this peak to the OH stretch from water molecules with bifurcated hydrogen bonds. This assignment also implies a molecular arrangement with a lower degree of hydrogen bond order than the OH-SS-S peak. We label this peak as the OH-SS-A peak. Since both OH-SS-A peak assignments imply a lower degree of hydrogen bond order than the OH-SS-S peak, the relative number of water molecules in an ice-like or a water-like arrangement can be determined through analysis of the VSFS spectra. A third peak located at 3680 cm^{-1} has been used by others[8,18] to study water molecules at the interface not involved in hydrogen bonding but has not been examined in these studies which focus exclusively on the hydrogen-bonded modes.

The red shift of the peak position of the OH peaks with increased intermolecular hydrogen bonding as is seen in the three aforementioned peaks has been thoroughly examined for bulk water.[20,25,26] The shift occurs because hydrogen bonding "steals" bond strength from the OH bond as the stronger hydrogen bonds weaken the OH covalent bond with a subsequent shift of the vibrational modes to lower energy. A comparison of the peak positions with the degree of hydrogen bonding illustrates the well-known trend that the peak position of the OH stretching mode is red-shifted with increasing hydrogen bonding. Accompanying the red shift of the peak frequency with increased hydrogen bonding is a large increase in the bandwidth of the OH stretch. This increase in the

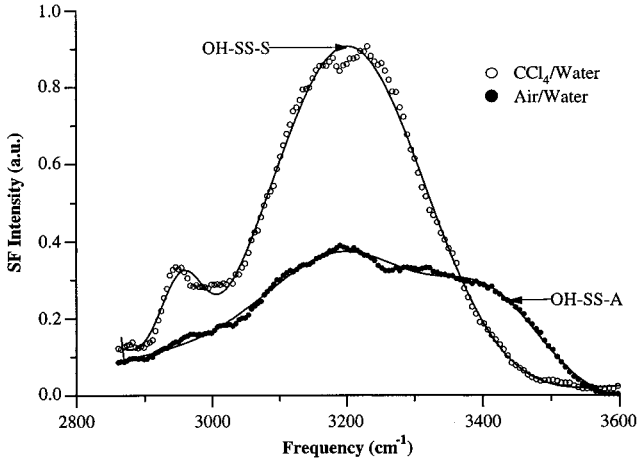

Figure 1. VSF spectra under S-sfg, S-vis, P-ir polarization conditions from the neat CCl_4/water (open circles) and air/water (filled circles) interfaces. Solid lines are a spectral fit to the data using eqs 1 and 3.

bandwidth results from dynamic dipole−dipole coupling between neighboring water molecules which produces a distribution of low- and high-frequency stretching modes.[20,25,26] The nature of this distribution also has an effect on the position of the peak frequency of the OH stretching mode. Deconvolution of these two effects, hydrogen bonding and intermolecular coupling, on the energetics of the OH stretching peaks in the vibrational spectra is difficult and generally requires the study of HOD in H_2O or D_2O which eliminates the intermolecular coupling effect. However, the extent of hydrogen bonding can be inferred through a comparison of the relative number of water molecules contributing to the ice-like and water-like peaks. This comparison is possible since the ice-like peak is indicative of more complete hydrogen bonding than the water-like peak.

Figure 1 shows the combined spectra of interfacial water taken at the neat air/water and CCl_4/water interfaces. For the former, both the OH-SS-S and the OH-SS-A peaks are observed with the more symmetrically bonded peak (ice-like peak) showing somewhat greater intensity. At the CCl_4/water interface, intensity is only observed from this ice-like peak at 3200 cm^{-1}. The small peak observed at approximately 2950 cm^{-1} in the VSFS spectrum from the CCl_4/water interface is a result of a very small amount of contaminant at the interface. This peak is observed in the CCl_4/water spectra and not in the spectra from the air/water interface because of the enhanced affinity amphiphilic molecules have for the CCl_4/water interface and the enhanced sensitivity we observe in the TIR geometry. In this geometry, surface concentrations as low as a thousandth of maximum surface coverage, which corresponds to a molecular area of approximately 1500 $Å^2$/molecule, can be measured.

What does this difference in spectral features suggest about the differing types of hydrogen bonding at these two interfaces if one assumes that the peaks observed are representative of water in these two different types of hydrogen-bonding structure? The relative number of water molecules contributing to each peak can be determined by taking the square root of the integrated area for each peak and dividing that into the sum of the square root of the integrated area for the two peaks. In isotopic dilution studies later to be described,[5,27] we show that the square root area under the OH peaks in the VSFG spectra of surface water is a good indicator of the relative number of oscillators (water molecules) contributing to the OH peaks. At the CCl_4/water interface we find that essentially all the hydrogen-bonded water molecules are in a tetrahedral arrangement similar to the structure of ice while at the air/water interface we find that only about 60% of the water molecules are in an ice-like arrangement with the remaining water molecules in a less hydrogen-bond-ordered, water-like arrangement. We attribute this difference in bonding character at the CCl_4/water interface to the ability of water to solvate a nonpolar molecule such as CCl_4 and the corresponding decrease in entropy associated with the solvation of nonpolar molecules. It is this decrease in the entropy of the system which overrides the enthalpy of solvation and causes the solvation of nonpolar molecules in water to be energetically unfavorable. The decrease in entropy is thought to result from water molecules rearranging into a tetrahedral structure in order to maximize hydrogen bonding in the presence of a nonpolar solute.[1,28] Our observation that the VSFS spectrum is dominated by the ice-like peak at the CCl_4/water interface is a direct manifestation of the structure-inducing influence of CCl_4 molecules on the interfacial water molecules. This observation is also consistent with previous calculations of hydrogen bonding at an oil/water interface which suggest that there is an increase in the strength of the hydrogen bonding among the water molecules near a hydrophobic surface.[29] At the air/water interface the water molecules are not influenced by the presence of a nonpolar molecule, and thus the water-like peak accompanies the ice-like peak. For the air/water interface the presence of the ice-like peak is a result of bulk termination which induces maximum formation of hydrogen bonds at the interface, and thus the tetrahedral structure is preferred. In Raman and IR studies of bulk ice, this OH-SS-S peak is dominant in this spectral region.

The VSFS spectrum that we have obtained from the air/water interface is in good agreement with previous VSFS work by Shen et al.[8,18] However, our CCl_4/water results differ from what they observe for the hexane/water interface which one might presume to show similar behavior. Instead, Shen et al. found that at the air/water and hexane/water interfaces the VSFS spectra were very similar in that there was nominally an equal distribution of intensity between the water-like and ice-like peaks. This observation differed from the quartz/octadecyltrichlorosilane (OTS)/water interface where they found that the VSFS spectrum was dominated by the ice-like peak. Their hexane/water studies were conducted by spreading a thin layer of hexane on the water surface and then recording a spectrum. For our studies at the CCl_4/water interface approximately 50 mL of water is placed on top of 180 mL of CCl_4. One might argue, as was done in explaining the difference observed between the hexane/water and the quartz/octadecyltrichlorosilane (OTS)/water studies,[8] that this difference between the air/water and the CCl_4/water interface is due to an increase in the rigidity due to the hydrostatic pressure of 50 mL of water pushing down on the interface, thus restricting the packing of the water molecules. This explanation however contradicts theoretical[29−31] and experimental[32,33] endeavors from which a high degree of interface roughness is inferred at these interfaces. Another possible explanation for the difference in hydrogen bonding observed at the CCl_4/water and hexane/water interfaces is that the different molecular shapes of CCl_4 and hexane influence the interfacial water structure. We have attempted to perform similar experiments using hexane and cyclohexane (both deuterated and hydrogenated) and have been unsuccessful in obtaining reliable spectra from these interfaces. The main experimental complication has been absorption of the IR light by the thin layer of alkane, thus rendering the IR light that reaches the interface too weak to produce a detectable VSFS response.

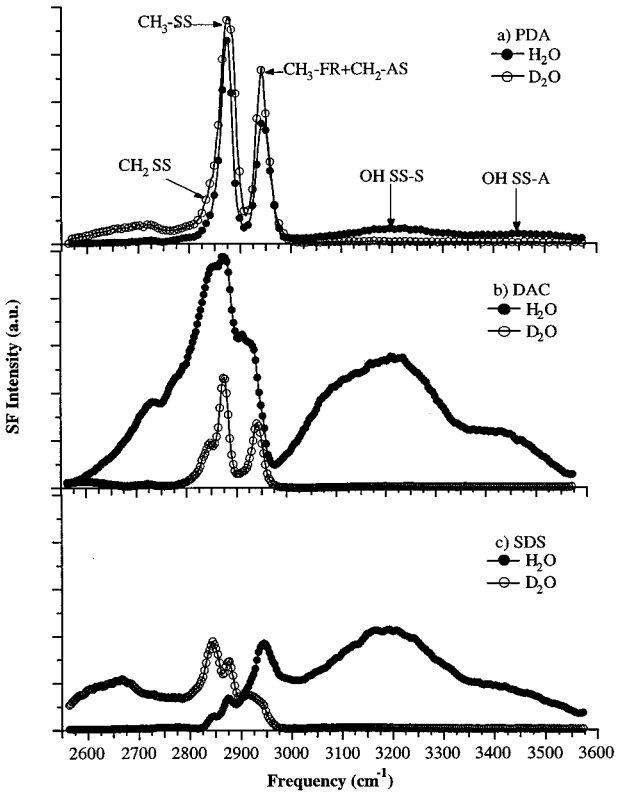

Figure 2. VSF spectra under S-sfg, S-vis, P-ir polarization conditions from the air/H_2O (filled circles) and D_2O (open circles) interfaces. (a) Monolayer (ca. 25 Å^2/molecule) of pentadecanoic acid (PDA), (b) 14 mM dodecylammonium chloride (DAC) solution, and (c) 8.1 mM sodium dodecyl sulfate (SDS) solution.

E. Effect of Adsorbed Surfactant at the Air/Water Interface

1. Headgroup Effects. Commercial surfactants have a broad range of uses in technology, environmental sciences, and oil recovery in addition to being components in a vast number of consumer products ranging from soaps and medicinal drugs to motor oils and cosmetics. Natural surfactants play a vital role in all aspects of biology and biochemical processes. The interaction between water and a charged surfactant often controls the behavior of the surfactant at a variety of interfaces including the surface of micellar, membranous vesicles.[1] At planar surfaces such as at the air/water and oil/water interface it is well-known that surfactants interact with surface water to significantly perturb the thermodynamic properties of that surface, most notably the surface tension. The focus of the studies described in this and the following section is to probe how the structure of surface water molecules is perturbed by the presence of surfactants and ions in the aqueous phase. Numerous studies have been published that investigate the structure of surfactants at both the air/water[6,10,34,35] and CCl_4/water[3,7] interfaces with the primary focus being on the alkyl chain structure of the surfactants as they adsorb to the interface. These are the first studies that have examined both the water and surfactant structure in parallel to obtain a more complete picture of the effect of surfactants on hydrogen bonding and water structure at aqueous interfaces.

Figure 2 shows the vibrational spectra from three different surfactants at the air/H_2O and air/D_2O interface. Figure 2a shows the vibrational spectra from a monolayer, approximately 25 Å^2/molecule, of the nonionic surfactant pentadecanoic acid (PDA)[36] while Figure 2b,c shows the vibrational spectra from the ionic surfactants dodecylammonium chloride (DAC cationic) and sodium dodecyl sulfate (SDS anionic) at their respective critical micelle concentrations. Films of PDA at the air/water interface have been studied previously by the VSFS technique and have been shown to readily form well-ordered monolayers, consistent with what is observed here.[10,34,35] Both spectra in Figure 2a are dominated by the CH_3 symmetric stretch, CH_3-SS at 2875 cm^{-1}, and the CH_3 Fermi resonance, CH_3-FR at 2935 cm^{-1}, with little or no contribution observed from CH_2 stretching modes. For amphiphilic molecules that form well-ordered monolayers, predominantly in an all-trans conformation, the CH_2 bonds will be on opposing sides of the carbon backbone. This orientation produces a cancellation of the CH_2 stretching vibrational modes, and thus a monolayer with no or few gauche defects will exhibit only CH_3 vibrational modes in the SF spectrum. Conversely, the presence of the CH_2 vibrational modes in a particular spectrum implies a lesser degree of order or more gauche defects. The dominance of the CH_3-SS over negligible contributions from the CH_2-SS for the PDA spectra suggests considerable ordering of the monolayer.

In addition to the CH stretching modes, we find two weak peaks in the PDA-H_2O spectrum at higher frequency which were previously not measured for this system. The first peak located at 3200 cm^{-1} is attributed to the ice-like peak (OH-SS-S) while the second peak located at 3400 cm^{-1} is attributed to the water-like peak (OH-SS-A). Both peaks were described in the previous section and result from the coupled OH vibrational modes of water molecules in a more hydrogen bonded and less hydrogen bonded environment, respectively. The corresponding OD peaks, in the 2600−2700 cm^{-1} range, are present in the spectrum of PDA on D_2O. However, since the IR power from the laser system is decreasing rapidly in this region, these peaks are not easily resolvable and will not be discussed further.

Figure 2b shows the VSFS spectra from the air/water interface of 14 mM dodecylammonium chloride solutions in both H_2O and D_2O. Upon comparison of the DAC-H_2O spectrum with the PDA-H_2O spectrum, one immediately notices in the DAC-H_2O spectrum a large enhancement of the OH peaks from the interfacial water molecules. This enhancement in the OH peaks is attributed to the large electrostatic field present in the double-layer region arising from separation of the cationic headgroup and chloride ions (present at the interface as counterions). At maximum surface coverage the electrostatic field can be as large as 10^8 V/m and extend into the bulk water as much as 100 water molecule diameters. This electrostatic field can align the dipole moments of the interfacial water molecules which has a twofold effect on the VSFS spectra in the OH stretching region. The first effect arises from removal of the inversion symmetry to a depth further into the bulk of the water than in the absence of an interfacial electrostatic field. This allows a greater number of water molecules to interact with the optical fields, thus producing an enhancement in the OH stretching peaks. The second effect results from alignment of the OH transition moments with the polarization vector of the IR laser beam. For a large electrostatic field where the dipoles of the water molecules are aligned the cancellation between OH transition moments is small, thus producing enhanced OH peaks. The observed enhancement is certainly a combination of each of these effects. These conclusions are consistent with those derived from nonresonant SHG studies of water molecules at the charged quartz/water interface[37] and the charged insoluble surfactant air/water interface.[12] The peak at 3200 cm^{-1} dominates over the peak at 3450 cm^{-1} in the DAC-H_2O spectrum which indicates a preference for the ice-like structure

of the interfacial water molecules. Another notable difference in the comparison of the PDA-H_2O and DAC-H_2O spectra is the dip in the DAC spectra at approximately 2970 cm^{-1} indicative of a destructive interference between the CH peaks and the OH-SS-S peak. This interference is not present in the DAC-D_2O spectrum which provides further evidence that the OH peaks are involved. An additional peak is observed near 2700 cm^{-1} in the DAC-H_2O and DAC-D_2O spectra which is likely due to an NH Fermi resonance.

Figure 2c shows the VSFS spectra from solutions of 8.1 mM SDS in H_2O and D_2O at the air/water interface. Inspection of the SDS-H_2O spectrum in the OH stretching region shows some similarities to the DAC-H_2O spectrum, namely, the OH peaks are greatly enhanced as a result of the field present in the double-layer region due this time to separation of the *negatively* charged headgroup of SDS and the *positively* charged sodium ions (present at the interface as counterions). In addition, like DAC, the OH peak at 3200 cm^{-1} dominates over the peak at 3450 cm^{-1}, indicating a preference for a tetrahedral arrangement of the interfacial water molecules in the presence of charged surfactant. Upon further inspection, however, one finds that the destructive interference in the DAC-H_2O spectrum located at 2970 cm^{-1} is replaced by an enhancement or constructive interference for the SDS-H_2O spectrum. In fact, the CH_3 Fermi resonance is enhanced so much that it now dominates the CH stretching spectral region. This situation is not observed for the SDS-D_2O spectrum which is dominated by the CH_2-SS and a much smaller signal from CH_3-FR. This behavior can be explained by the electrostatic fields present at these interfaces which are in opposite directions for DAC and SDS. The fields will align the dipoles of the interfacial water molecules in opposite directions, and thus the OH stretching modes will have moments in opposite directions. The difference in directionality of the OH bonds for the two surfactants gives rise to the difference in the interference between the CH modes and the OH-SS-S peak at 3200 cm^{-1}. Specifically, for SDS, constructive interference, the methyl and water transition dipoles are pointed in the same direction whereas for DAC, destructive interference, the transition dipoles are pointed in opposite directions. Assuming that the methyl transition dipole moments are in the same direction for DAC and SDS leads one to conclude that it is the water transition dipole that flips with the sign of the charged surfactant layer. This flip in the molecular arrangement of interfacial water molecules at oppositely charged surfaces has been observed at the charged electrode/water interface with X-ray scattering experiments[38,39] and proposed to occur at the charged insoluble surfactant air/water interface by SHG experiments.[12]

Another possible contributing factor in the interfacial water alignment could arise from the chemical nature of the solvation shell of the charged headgroup. While this type of alignment certainly occurs in the solvation sphere of the charged headgroups, one would expect these effects to align only the water molecules in the double-layer region neighboring the surfactant headgroups. Since the alignment of so few water molecules would probably not produce the large enhancements observed here, we conclude that the dominate contribution in these studies is the field-induced orientation. More evidence for this will be presented below with studies involving mixed cationic and anionic surfactants.

If the enhancement in the OH spectral region observed in the spectra from both DAC and SDS is due to the electrostatic field at the interface, then at an interface where the electrostatic field is zero, the enhancement should disappear. One means

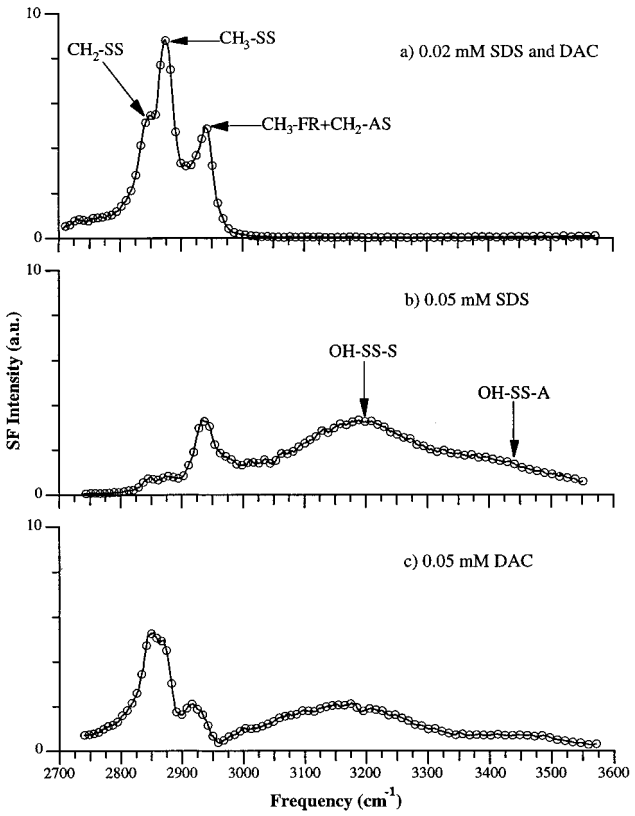

Figure 3. (a) VSF spectra under S-sfg, S-vis, P-ir polarization conditions from the air/water interface of an aqueous solution of (a) both 0.02 mM DAC and 0.02 mM SDS, (b) 0.05 mM DAC, and (c) 0.05 mM SDS. Solid lines are a guide to the eye.

of testing this is through examination of an interface where there are approximately equal numbers of cationic and anionic surfactant molecules. Figure 3a shows the SSP VSFS spectra from the air/water interface of a solution containing both 0.02 mM DAC and 0.02 mM SDS. The OH peaks are not present in this spectrum which is consistent with the lack of a large electrostatic field present at the interface. For comparison with the mixed surfactant case, parts b and c of Figure 3 show the SSP VSFS spectra from 0.05 mM SDS and DAC solutions, respectively. In both the 0.05 mM SDS and DAC VSFS spectra the OH peaks are quite prominent. The disappearance of the OH peaks in the spectra from the mixed surfactant system is attributed to the cancellation of charge between the cationic and anionic surfactants and oppositely charged counterions present in the double-layer region. The cancellation of surface charge leads to a much smaller field present at the interface, and thus the interfacial water molecules are no longer preferentially aligned.

2. Electrostatic Field Effects. The interfacial electrostatic field accompanying the presence of charged surfactant not only aligns the interfacial water molecules but also affects the intermolecular hydrogen bonding. The effects of the electrostatic field on the intermolecular hydrogen bonding are probed by comparing the relative number of OH oscillators contributing to each peak in the VSFS spectra.[40] Figure 4 shows the VSFS spectra from water molecules at the air/water interface with varying bulk concentrations of SDS and an ionic strength of 10 mM. Detuerated SDS is used to simplify the deconvolution of the OH peaks. The solid lines in Figure 4 are a fit to the data using eqs 1 and 3 from which we obtain the position, area, width, and intensity of each peak. As the bulk concentration is increased, we observe an enhancement in the OH peaks from

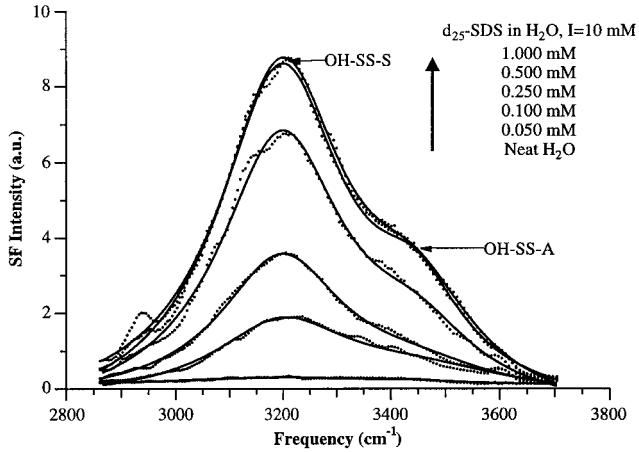

Figure 4. VSF spectra from the air/water interface under S-sf, S-vis, P-ir polarization conditions for various bulk concentrations of deuterated SDS and an ionic strength of 10 mM. Solid lines are a least-squares fit to the data using eqs 1 and 3.

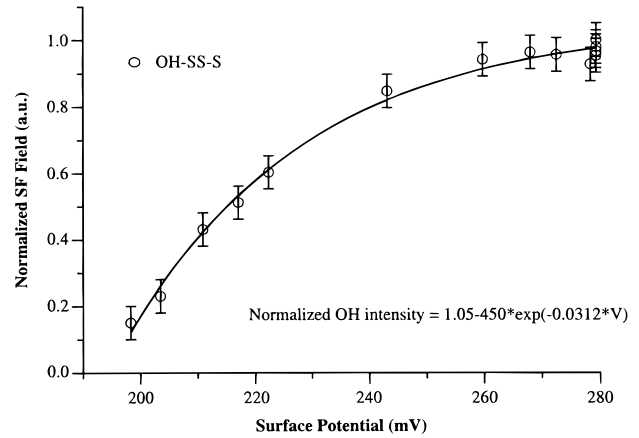

Figure 5. Normalized SF field at the position of the OH-SS-S peak from the fitted spectra in Figure 4 plotted as a function of the surface potential for the air/water interface. Surface potential was determined from surface tension measurements and the Gibbs and Gouy−Chapman equations. Solid line is a least-squares fit to the data using an exponential function with the functionality included in the figure.

the interfacial water molecules. As mentioned above, this enhancement is a result of the alignment of the interfacial water molecules which accompanies the interfacial electrostatic field produced by the charged surfactant. We observe this enhancement at bulk concentrations corresponding to very small surface coverages, approximately 200−300 Å^2/molecule, and find that a maximum in the enhancement is observed well before the maximum surface coverage is reached at 2−3 mM. This first observation illustrates the high sensitivity of VSFS to the presence of charged surfactants at the interface, and from the second observation we infer that the interfacial water molecules achieve their greatest degree of alignment before maximum surface coverage is attained.[40]

To further examine this latter point, the SF field at the position of the OH-SS-S peak, normalized to unity at maximum intensity, is plotted in Figure 5 as a function of the surface potential calculated from surface tension measurements. From Figure 5 we find that the SF field reaches a maximum at a surface potential of approximately 260 mV. Equation 6 would predict that the SF field should be linear with the surface potential where we find that the SF field has an exponential dependence on the surface potential. This deviation from linearity is a result of the alignment of the dipole moments of the interfacial water

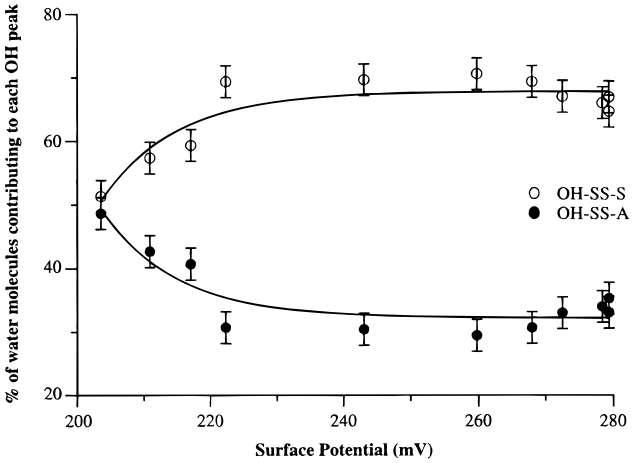

Figure 6. Relative percent of the OH oscillators contributing to each OH peak as determined from the fitted spectra in Figure 4 plotted versus the surface potential. Solid line is a least-squares fit to the data using an exponential function.

molecules which results in a lesser degree of cancellation of the transition moments of the OH stretches as the surface potential increases. The maximum enhancement observed at 260 mV then corresponds to maximum alignment of the interfacial water molecules with further increases in the potential having minimal effect on the alignment of the water molecules. Potential-dependent alignment of the interfacial water molecules has been observed previously at the charged electrode/water interface with FTIR[41,42] and X-ray scattering experiments.[38,39]

From the two peaks present in the spectra of Figure 4 we can obtain information concerning the hydrogen bonding between interfacial water molecules in the presence of charged surfactant at the air/water interface. As was mentioned earlier, the first peak at 3200 cm^{-1} is attributed to the in-phase coupled OH stretching modes from water molecules that are in a tetrahedral arrangement with a high degree of hydrogen bond order while the peak located between 3400 and 3450 cm^{-1} is attributed to OH stretches from water molecules that have incomplete tetrahedral coordination and a lesser degree of hydrogen bonding. Further, we have shown through isotopic dilution studies[5,27] that the square root area under the OH peaks in the VSFG spectra of surface water is a good indicator of the relative number of oscillators (water molecules) contributing to the OH peaks. Figure 6 shows the relative percent of OH oscillators contributing to each peak calculated from the fitted areas from Figure 4 plotted versus the surface potential. Figure 6 shows that there is an increase in the extent of hydrogen bonding accompanying an increase in the surface potential. In fact, the partitioning of water molecules into the more hydrogen bond ordered structure increases from 50% at approximately 200 mV to 70% at approximately 230 mV.

Figure 7 shows the VSFS spectra from the air/water interface for a 4.00 mM bulk SDS concentration at varying ionic strengths. The solid lines in Figure 7 are a fit to the data using eqs 1 and 3. As the ionic strength is increased from 4.00 mM to 0.5 M, we observe a dramatic decrease in the enhanced OH peaks in the VSFS spectra. The decrease in the enhancement with increasing ionic strength results from both a decrease in the surface potential and a decrease in the double layer depth. The decreased surface potential diminishes the alignment of the interfacial water molecules while the decreased double-layer depth reduces the number of water molecules interacting with the optical fields. The range of ionic strengths studied results in the double-layer changing from a few angstroms to a few

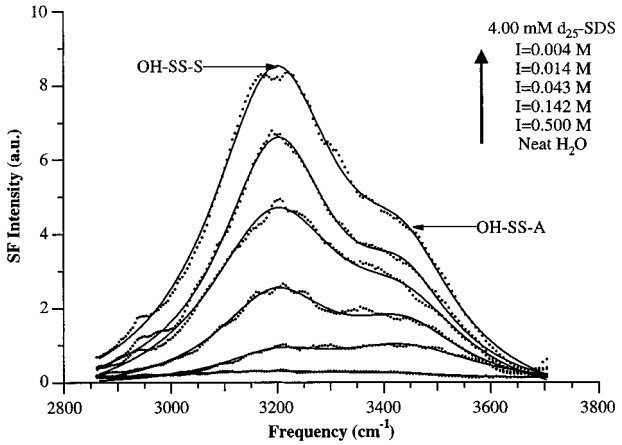

Figure 7. VSF spectra from the air/water interface under S-sf, S-vis, P-ir polarization conditions for various ionic strength and a bulk SDS concentration of 4.00 mM. Solid lines are a least-squares fit to the data using eqs 1 and 3.

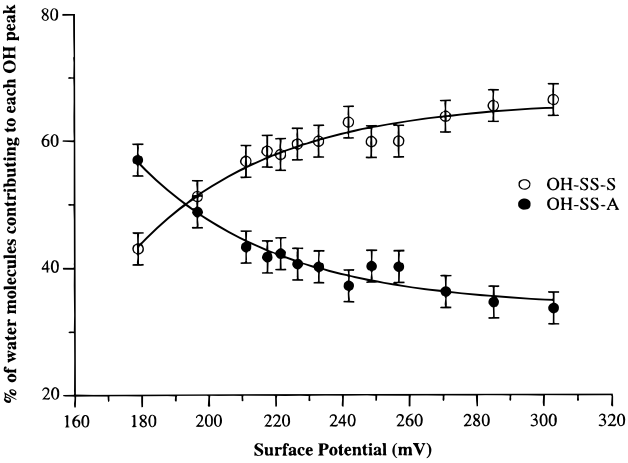

Figure 8. Relative percent of the OH oscillators contributing to each OH peak as determined from the fitted spectra in Figure 7 plotted versus the surface potential. Solid line is a least-squares fit to the data using an exponential function.

nanometers, which corresponds to a variation from a few water layers to tens of water layers. Figure 8 shows the relative percent of OH oscillators contributing to each peak calculated from the fitted data in Figure 7 plotted versus the surface potential determined from surface tension measurements. As the interfacial potential is increased by decreasing the ionic strength, Figure 8 shows that there is a progression from a less hydrogen bond ordered structure to a more hydrogen bond ordered structure. The partitioning of water molecules into the more hydrogen bond ordered structure increases from 40% at approximately 180 mV to 65% at approximately 230 mV, which is in good agreement with the similar data in Figure 6 obtained by varying the bulk concentration.

The presence of charged surfactant at the air/water interface induces an electrostatic field in the double-layer region. This field is on the order of 10^8 V/m at maximum surface coverage and can induce an alignment of the interfacial water molecules which is manifested in the VSFS spectra. The depth of the field and thus the region probed by VSFS is on the order of the double layer which, within the confines of Gouy−Chapmann theory, depends on the solution ionic strength. The dependence of the SF field in the OH stretching region on the surface potential is illustrated in Figure 5. As the surface potential is increased by increasing the bulk concentration of SDS while holding the ionic strength constant at 10 mM, we observe an increase in the SF field at the position of the OH-SS-S peak. The functionality of this increase follows an exponential, which agrees well with previous experiments conducted at the metal electrode/water interface.[41,42] At the air/water interface we find that the interfacial water molecules attain the highest degree of alignment at a potential of 260 mV whereas for the metal electrode/water interface maximum alignment was observed at a potential of 500 mV. The difference in the potential at which maximum alignment is achieved at the SDS−air/water interface in comparison to the metal electrode/water interface is possibly due to extended hydrogen bonding between the interfacial water molecules and the SDS headgroup. At the SDS−air/water interface the water molecules are oriented by the electrostatic field with their hydrogens pointed toward the air. Hydrogen bonding between SDS headgroups and water molecules aligns the water molecules such that the hydrogens are directed toward the headgroup, which is essentially the same orientation produced by field alignment. Extended hydrogen bonding between water molecules and the SDS headgroups would act to enhance the field alignment of the interfacial water molecules, thus causing maximum alignment to occur at a lower surface potential. Hydrogen bonding of the water molecules in the solvation sphere of the surfactant headgroup also may contribute to the enhancement. However, theoretical studies of SDS at the air/water and CCl_4/water interfaces have shown that these waters are contained within several angstroms from the headgroup whereas the double-layer region extends several nanometers and thus contains many more water molecules.[43] The fact that there are fewer water molecules in the solvation sphere means that the dominant contribution to the enhanced SF response arises from water molecules not necessarily participating in solvation of the headgroup.

Figures 6 and 8 illustrate how the intermolecular hydrogen bonding changes as a function of the surface potential at the air/water interface. The observed increase in the relative percent of oscillators contributing to the more strongly hydrogen bonded peak (OH-SS-S) with increasing surface potential provides us with direct evidence that the intermolecular hydrogen bonding increases with increasing surface potential. Theoretical studies of water molecules between two platinum electrodes with surface charge densities covering the same range of values as those determined here from the SDS−air/water interface have shown a similar trend.[44−46] We observe this trend in two separate cases: first by increasing bulk SDS concentration to increase the surface potential (Figure 6) and second by decreasing the ionic strength to increase the surface potential (Figure 8). The functionality shown in the two figures is somewhat different with the plot in Figure 6 rising at a faster rate than the plot in Figure 8. This phenomenon is due to the fact that as the ionic strength is varied (Figure 8) *both* the surface potential *and* the double-layer depth change. In contrast, as the bulk surfactant concentration is varied (Figure 6) at constant ionic strength only the surface potential changes. Low surface potentials in Figure 8 correspond to high ionic strength and thus a small double layer, thereby producing a larger electrostatic field and greater alignment than the equivalent surface potential in Figure 6. Complicating the situation even more is the fact that as the double layer decreases with decreasing ionic strength there are fewer water molecules interacting with the optical fields. We have had little success deconvoluting each effect in the data in Figure 8; thus, the data are presented as a function of the surface potential and only qualitatively compared to Figure 6.

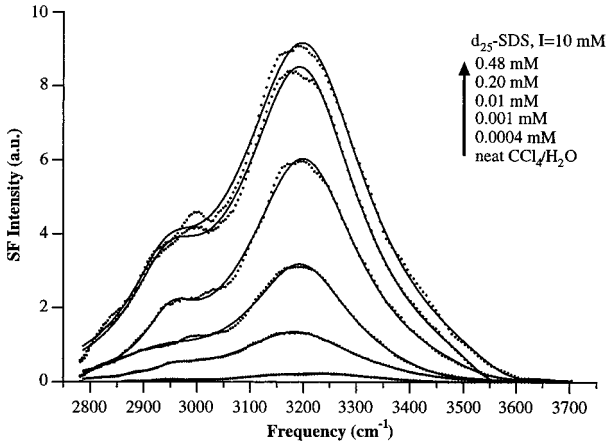

Figure 9. VSF spectra from the CCl_4/water interface under S-sf, S-vis, P-ir polarization conditions for various bulk concentrations of SDS and an ionic strength of 10 mM. Solid lines are a least-squares fit to the data using eqs 1 and 3.

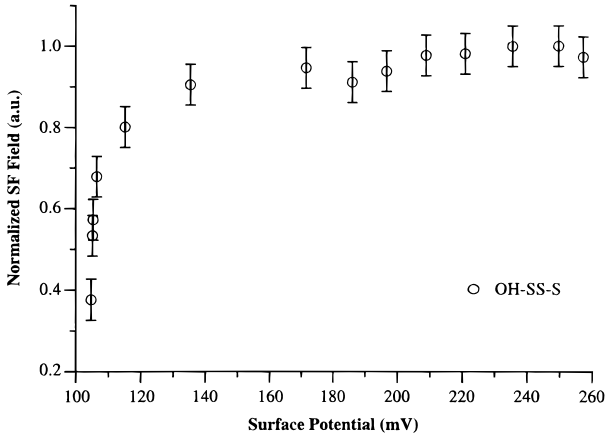

Figure 10. Normalized SF field at the position of the OH-SS-S peak from the fitted data of Figure 9 plotted versus the interfacial potential. The interfacial potential is calculated from surface tension measurements and the Gibbs equation.

X-ray scattering experiments[38,39] of the electrode/water interface suggest that there is a substantial increase in the density of interfacial water molecules as compared to bulk water caused by destruction of the hydrogen-bonded network when a large electrostatic field is applied across the interface. The work presented here as well as theoretical studies[44,45] shows the opposite behavior in that there is actually an increase in the intermolecular hydrogen bonding when a large electrostatic field is applied across the interface. This observation is inferred from Figures 6 and 8 which show that as the interfacial potential is increased the partitioning into the more extensively hydrogen-bonded ice-like peak also increases. A possible explanation for the increased hydrogen bonding observed in the SFG studies presented here and the increased density observed in X-ray studies arises from the structure of the aligned dipoles of the water molecules. Specifically, it seems possible that the highly aligned interfacial water molecules may adopt a structure in which both the hydrogen bonding and the density are increased with respect to the bulk properties. Further inspection of Figures 6 and 8 shows that a maximum in the partitioning of water molecules into the more hydrogen bond ordered structure occurs at approximately 230 mV. The fact that this potential is somewhat smaller than the 260 mV potential required to achieve maximum alignment of the water dipoles as shown in Figure 5 shows that increased dipole alignment with increased surface potential may continue to occur after maximum hydrogen bonding is achieved.

F. Effect of Adsorbed Surfactant at the CCl_4/Water Interface

Figure 9 shows the VSFS spectra from the CCl_4/H_2O interface in the OH stretching spectral region with varying bulk concentrations of the charged soluble surfactant SDS (deuterated) present in the aqueous phase and an ionic strength of 10 mM. Inspection of the spectra in Figure 9 shows that similar to the air/water case there is a large enhancement in the intensity from the OH peaks as the bulk surfactant concentration is increased. This increase with increasing bulk concentration is again a result of the fact that the interfacial concentration, and thus the surface charge density and magnitude of the electrostatic field, is a function of the bulk surfactant concentration. We find that this enhancement reaches a maximum value at a bulk concentration of approximately 0.5 mM while surface tension measurements show that the maximum surface coverage of the surfactant occurs around 1−2 mM.[40] From this observation we infer that the water molecules have achieved their highest degree of alignment before maximum surface coverage is reached. Further, the onset of this enhancement of the OH peak is observed several orders of magnitude below the maximum surface concentration, at submicromolar bulk surface concentrations. The ability to detect a very low surface concentration of SDS again illustrates the high sensitivity of the TIR geometry in making VSFS measurements.

Inspection of Figure 9 shows that the dominant feature in the VSFS spectra from the CCl_4/water interface in the presence of SDS is the OH-SS-S (ice-like) peak while there is little or no evidence for intensity from the OH-SS-A (water-like) peak.[19] This observation is markedly different from what was observed at the air/water interface where the water-like (OH-SS-A) peak gave rise to a prominent shoulder on the ice-like (OH-SS-S) peak. The shoulder in the 2900−3050 cm^{-1} region in the spectra from Figure 9 arises from a small amount of contaminant, CH stretches, present at the neat interface riding on the large OH-SS-S peak. From the dominance of the OH-SS-S peak we infer that the prevailing structure of water molecules at the CCl_4/water interface in the presence of SDS is a tetrahedral arrangement much like the structure of ice. The similarity of the water structure at the CCl_4/water interface both in the presence and in the absence of a charged soluble surfactant further allows us to infer that the presence of the surfactant and counterions in the aqueous phase does not disrupt to any measurable extent the hydrogen bond ordering of the interfacial water molecules.

Figure 10 shows the normalized SF field from the OH-SS-S peak obtained from the spectra in Figure 9 plotted against the interfacial potential determined from surface tension measurements.[40] As was the case for the air/water data, we find that at the CCl_4/water interface the dependence of the SF field on the interfacial potential deviates from the linear relationship predicted by eq 6. Again this deviation is a result of the alignment of the transition dipole moments of the interfacial water molecules with the polarization vector of the IR light. At the CCl_4/water interface we find that the water molecules achieve their maximum alignment at an interfacial potential of approximately 160 mV, somewhat below what was observed from the air/water interface.

G. Temperature-Dependent Studies

How the interfacial water structure varies with temperature in the presence of charged surfactant has been a focus of another

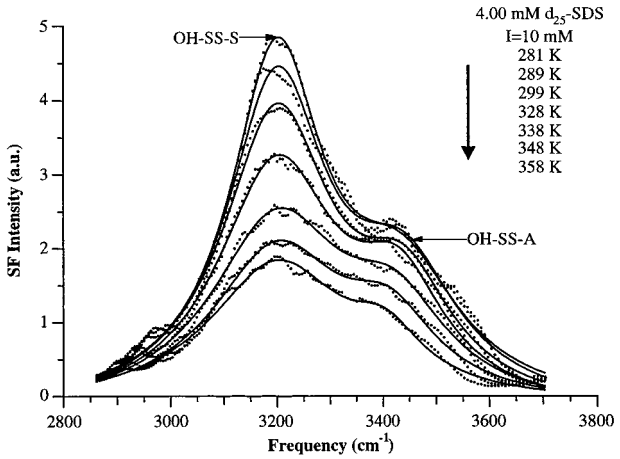

Figure 11. VSF spectra from the air/water interface under S-sf, S-vis, P-ir polarization conditions for various temperatures and a bulk SDS concentration of 4.00 mM and an ionic strength of 10 mM. Solid lines are a least-squares fit to the data using eqs 1 and 3.

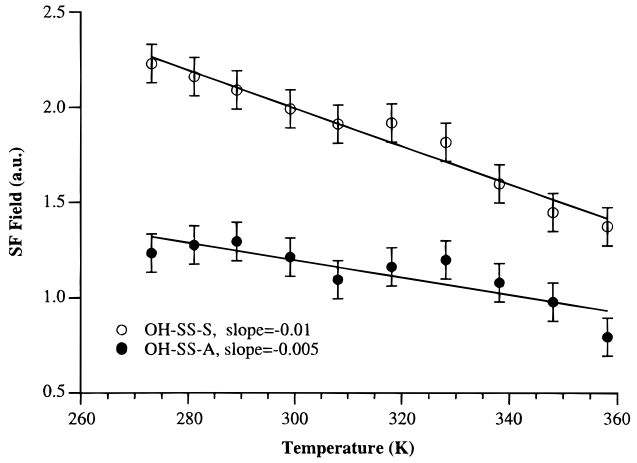

Figure 12. SF field at the position of the OH-SS-S peak from the fitted spectra in Figure 11 plotted as a function of the temperature. Solid lines are a linear least-squares fit to the data.

set of studies conducted at both the air/water and CCl_4/water interface. Figure 11 shows the VSFS spectra from the air/water interface with a bulk SDS concentration of 4.00 mM and an ionic strength of 10 mM for varying temperatures.[40] The spectra in Figure 11 show that the intensities of the OH peaks are very dependent upon the temperature. It is important to note that the spectra at temperatures above room temperature were obtained with a scan time of less than 1 min and were reproduced numerous times so that evaporation had no effect on the measured spectra. The decrease in the intensity of the OH peaks with increasing temperature results from the increased randomization of the interfacial water molecules afforded by the increased thermal energy. Figure 12 shows the SF field at the peak positions of the OH-SS-S and OH-SS-A peaks obtained by taking the square root of the peak intensity from the fitted spectra in Figure 11, plotted as a function of the temperature. These data illustrate the temperature dependence of the OH peaks, and the steeper slope obtained for the OH-SS-S peak implies that this peak is more temperature dependent than the OH-SS-A peak. Figure 13a shows the relative percent of OH oscillators contributing to each peak calculated from the fitted data in Figure 11 plotted versus the temperature. As the temperature is increased from near freezing to near boiling, we observe very little change in the partitioning of water molecules between the two peaks with the relative percent of oscillators

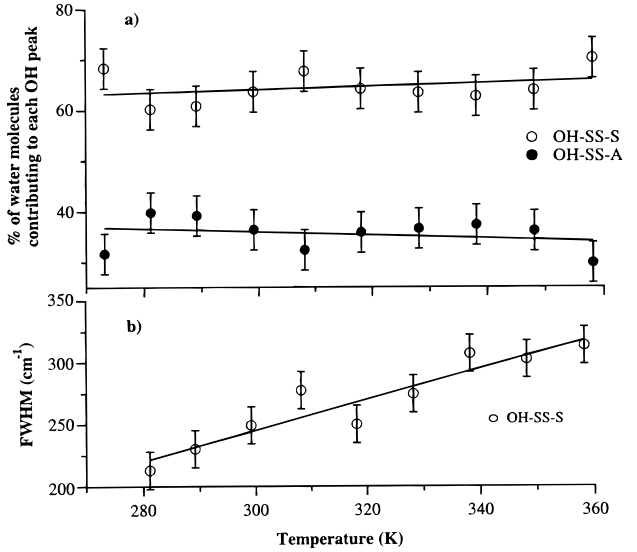

Figure 13. (a) Relative percent of the OH oscillators contributing to each OH peak as determined from the fitted spectra in Figure 11 and (b) fwhm of the OH-SS-S peak from the fitted spectra in Figure 11 plotted versus temperature. Solid lines are a linear least-squares fit to the data.

in each peak remaining constant at approximately 65% and 35% for the OH-SS-S and OH-SS-A peaks, respectively. The observation that the SF field at the OH peak positions decreases with increasing temperature whereas the partitioning between the ice-like and water-like peaks remains constant is a result of the increasing bandwidth of the OH peaks with increasing temperature as shown in Figure 13b. As the temperature is increased, the OH-SS-S peak intensity decreases while the bandwidth increases; these opposing effects cause the relative area of the OH-SS-S peak to remain constant. The increased bandwidth is a result of more states energetically accessible to the interfacial water molecules but still within the two OH stretching peaks. Thus, the relative number of water molecules contributing to each peak does not change; however, the distribution of environments in which the water molecules exist does change. The spectral broadening of vibrational modes with increasing temperature is well-studied[20−22] and results from a decrease in the net alignment of the transition dipole moments of the molecules with the polarization vector of the optical field. We see a similar effect occurs in the OH-SS-A peak but to a much lesser degree since the decrease in peak intensity is much smaller. Equation 7 shows that the surface potential increases with increasing temperature; thus, the fact that the SF field decreases with increasing temperature provides evidence that the increased randomization of interfacial water molecules by the increased thermal energy outweighs any alignment produced by increased surface potential. Surface tension measurements show that the surface tension remains relatively constant over the entire temperature range studied with a small decrease at the lowest temperatures.

Figure 14 shows the SF field at the OH-SS-S position from VSFS spectra of the SDS−CCl_4/water interface plotted versus the temperature. The temperature dependence of the OH-SS-S peak at the CCl_4/water interface is larger than both the OH-SS-S and OH-SS-A peaks at the air/water interface as evidenced by the larger slope shown in Figure 14 compared to the slopes shown in Figure 12. Earlier, we concluded that the intermolecular hydrogen bonding was more extensive at the CCl_4/water interface than at the air/water interface. The observation that the OH-SS-S peak from the CCl_4/water interface is more

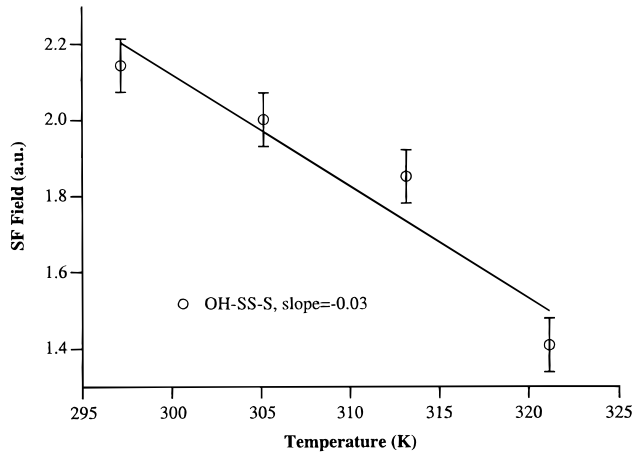

Figure 14. SF field at the OH-SS-S peak position from fitted VSF spectra from the CCl_4/SDS/water system plotted versus the temperature. Solid line is a linear least-squares fit to the data.

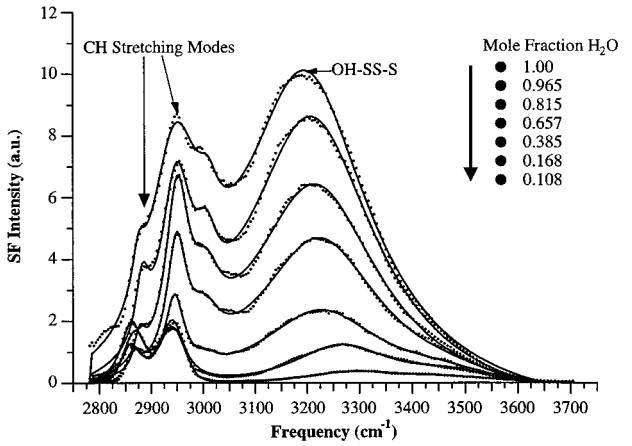

Figure 15. VSFG spectra from the CCl_4/SDS/H_2O interface with 1.0 mM SDS in the aqueous phase as a function of mole fraction of H_2O under S-sf, S-vis, P-ir polarization conditions.

temperature sensitive than from the air/water interface and the fact that hydrogen bonding is highly temperature sensitive provide further support that the intermolecular hydrogen bonding is greatest at the CCl_4/water interface. Previous VSFS measurements from the neat air/water interface show little or no temperature dependence in all of the OH peaks.[18] At both the air/water and the CCl_4/water interfaces in the presence of SDS we observe that the OH peaks are dependent on temperature. The observed temperature dependence at both interfaces in the presence of SDS, as compared to the lack of temperature dependence at the neat air/water interface, is a result of the high degree of alignment of the water molecules in the presence of SDS. For the case of the air/water interface the ice-like and water-like peaks have somewhat different temperature dependencies. From the slopes of the linear fits to the data in Figure 12, we conclude that the ice-like peak is more temperature dependent while the water-like peak is less temperature dependent following the trend predicted by the degree of hydrogen bonding.

H. Isotopic Dilution Studies

In the set of studies described in this section, we demonstrate the feasibility for using isotopic dilution studies to examine further the structure and hydrogen bonding at the CCl_4/H_2O interface in the presence of surfactants. This is the first time that isotopic dilution studies have been employed to examine hydrogen bonding at water surfaces. The studies lay the groundwork for future studies to be pursued in this area.[5,27] These initial studies have focused on the surfactant/CCl_4/H_2O interface as we seek to build on our understanding of this interface as described in previous sections.

Numerous IR and Raman studies of H_2O/D_2O mixtures have been conducted in the past to gain a better understanding of the structure of water in both bulk liquid water and bulk ice.[22,47−52] Referred to as isotopic dilution studies, such experiments have provided a wealth of information about hydrogen bonding of water molecules in terms of the inter- and intramolecular coupling between water molecules. The reasoning behind these studies is that as D_2O (H_2O) is added to H_2O (D_2O) the intermolecular coupling between the OH (OD) oscillators decreases as a result the difference in energy of the OH and OD stretches and to a lesser extent as a result of the difference in hydrogen bonding between H_2O and D_2O. The intermolecular decoupling as D_2O (H_2O) is added to H_2O (D_2O) manifests itself in the IR and Raman spectra as a blue shift in the spectral position of the OH (OD) stretching vibrations. This blue shift occurs as the mole fraction of H_2O (D_2O) is decreased and is a result of the decreased intermolecular coupling of the OH stretches between neighboring H_2O molecules. Experiments conducted on both cubic and amorphous ice have shown a blue shift in the OH-SS-S peak of approximately 100−120 cm^{-1} as the mole fraction of H_2O varies from 1.00 to 0.01 with the peak position of the OH stretch converging on the uncoupled mode at 3225 cm^{-1}.[49,51] In an effort to further characterize the structure of water molecules at the CCl_4/water interface in the presence of charged surfactants, we have conducted VSFS experiments on mixtures of H_2O and D_2O to probe the hydrogen bonding of interfacial water molecules.

Figure 15 shows the VSFS spectra from the CCl_4/water interface for various mixtures of H_2O and D_2O ranging from a H_2O mole fraction of 1.00 to 0.1 in the presence of the charged soluble surfactant SDS held constant at a bulk concentration and ionic strength of 1.00 mM. The mole fraction of H_2O was calculated assuming complete isotopic exchange and the equilibrium $H_2O + D_2O = 2HOD$ with $K = 4$.[47,52] For Figure 15 we have used hydrogenated SDS, and the CH stretching modes are indicated on the spectra. The shoulder in the spectra located at approximately 3000 cm^{-1} could be due to the OH stretch from water molecules that are hydrogen bonded to the charged sulfate headgroup with the large red shift presumably a result of the strong hydrogen bond. We have also observed a shoulder in this region from surfactants with sulfonate headgroups. We observe intensity in this spectral region from the deuterated SDS studies as well, but strangely we have not observed the shoulder in air/water studies with surfactants with either headgroup. The solid lines in Figure 15 are a least-squares fit to the data using eqs 1 and 3 from which we are able to extract peak intensities, positions, bandwidths, and integrated areas. Further, the intensities, positions, and bandwidths were all adjustable parameters in the fitting routine. We fit each spectrum to five peaks: two due to CH stretching modes, two due to OH stretching modes, and the last being the aforementioned peak at approximately 3000 cm^{-1}.

Inspection of Figure 15 shows that as the mole fraction of H_2O is decreased by adding D_2O there is a corresponding decrease in the intensity of the OH-SS-S peak resulting from fewer H_2O molecules contributing to the SF signal. For linear spectroscopies the integrated area of a particular peak is proportional to the number of oscillators contributing to that peak. For the case of VSFS the SF response is proportional to the square of the number of oscillators contributing to the signal;

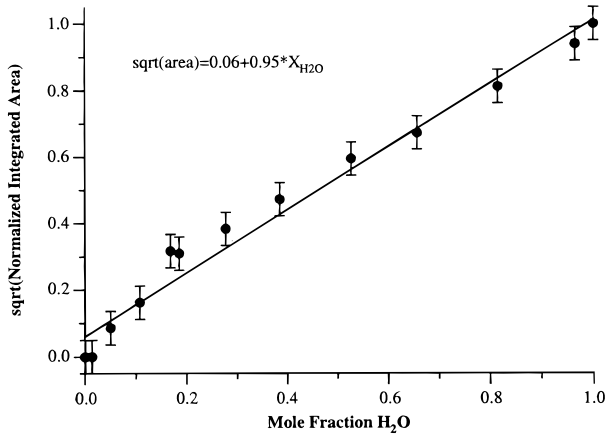

Figure 16. Plot of the square root of the normalized integrated area of the OH-SS-S peak from the data in Figure 15, determined from fits to eqs 1 and 3, as a function of the mole fraction of H_2O. Solid line is a linear fit to the data.

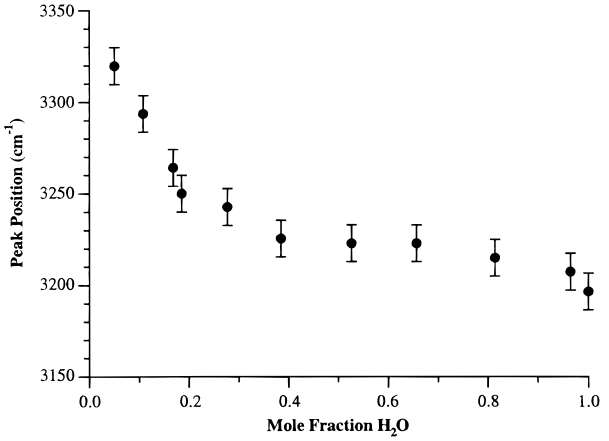

Figure 17. Peak position of the OH-SS-S peak from the data in Figure 15 plotted as a function of the mole fraction of H_2O. The data were fitted according to eqs 1 and 3.

thus, within the confines of eqs 1 and 3 the number of interfacial H_2O molecules contributing to the OH-SS-S peak is proportional to the square root of the integrated area for the OH-SS-S peak. Figure 16 shows a plot of the square root of the integrated area versus the mole fraction of H_2O where the square root of the integrated area has been normalized to unity for a H_2O mole fraction of unity. The solid line in Figure 16 is a linear fit to the data with the functionality expressed on the graph. The linear dependence of the square root of the integrated area on the mole fraction of H_2O shows that the square root of the area is a good measure of the relative number of oscillators contributing to the OH-SS-S peak in the VSFS spectra.

Close inspection of the spectra in Figure 15 shows that we are sensitive to the expected blue shift of the OH-SS-S peak position with decreasing H_2O mole fraction. The peak position goes from a value of 3200 cm^{-1} at a mole fraction of 1.00 to a value of 3320 cm^{-1} at a mole fraction of 0.05. The blue shift in the peak frequency of the OH-SS-S peak with decreasing H_2O mole fraction is a result of the intermolecular decoupling of the OH oscillators by the addition of OD oscillators as previously mentioned. The magnitude of the blue shift that we observe for H_2O molecules at the CCl_4/water interface in the presence of SDS is approximately the same, 120 cm^{-1}, as has been observed for both bulk amorphous ice and cubic ice[49,51] as well as supercooled water at -5 °C.[26] From this similarity we infer that the water molecules at the CCl_4/water interface are indeed very much in an ice-like arrangement with a high degree of hydrogen bond order and tetrahedral coordination. Figure 17 shows the peak frequency of the OH-SS-S peak obtained from the fits to the spectral data using eqs 1 and 3 plotted as a function of the mole fraction of H_2O. From Figure 17 we see that the peak frequency of the OH-SS-S peak blue shifts in nominally a linear fashion with decreasing H_2O mole fraction over the range from 1.0 to 0.2. Below a mole fraction of 0.2 the slope of the frequency shift with decreased H_2O becomes significantly steeper. This observation is most likely due to the increased HOD component present at the interface, resulting in an interference between OH peaks from HOD and H_2O and thus interfering with accurate fitting of the spectra.

Along with the uncoupling of the OH stretching modes that occurs as D_2O is added to H_2O, one also expects that HOD will be produced. Numerous IR and Raman spectroscopic studies have been performed on isotopic solutions of HOD in H_2O and D_2O in bulk liquid water and ice forms.[47−49,53] The reason for these studies is the simplified spectrum of HOD as

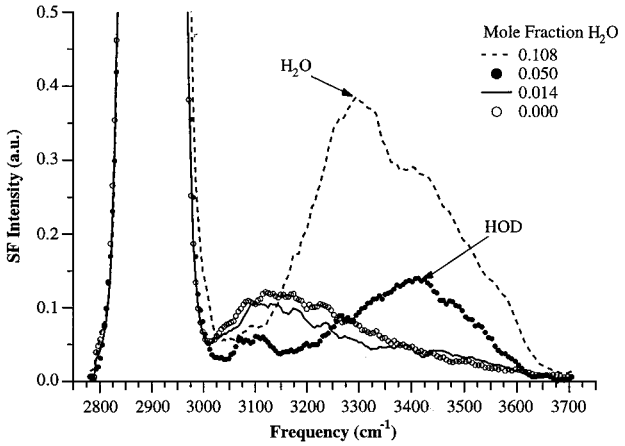

Figure 18. VSF spectra from the CCl_4/SDS/H_2O interface with 1.0 mM SDS in the aqueous phase for low mole fractions of H_2O under S-sf, S-vis, P-ir polarization conditions.

compared to that of H_2O or D_2O. This simplification is a result of two main factors: first the OH (OD) stretching mode of HOD in D_2O (H_2O) is intermolecularly uncoupled due to the dilution of the strong interaction between neighboring oscillators with bending and stretching modes overlapping in energy, and second the OH and OD stretching modes of HOD are intramolecularly uncoupled due to the isotopic mass difference. The fact that HOD is both intermolecularly and intramolecularly uncoupled simplifies the interpretation of the vibrational spectrum. A result of this simplification is that the vibrational spectrum of HOD in both H_2O and D_2O can been used by researchers to elucidate structural characteristics of bulk liquid water and solid ice. Figure 18 shows the VSFS spectra from the lowest mole fraction H_2O solutions studied with the SF intensity axis expanded so the OH features can be more easily discerned. From inspection of the 0.108 mole fraction H_2O solution spectra we observe a small shoulder at approximately 3460 cm^{-1} on the high-frequency side of the blue-shifted OH-SS-S peak from interfacial H_2O molecules. We attribute this peak at approximately 3460 cm^{-1} to the uncoupled OH stretch (OH-S) from interfacial HOD molecules produced by isotopic exchange between H_2O and D_2O. The VSFS spectrum from the 0.05 mole fraction H_2O solution shows that this peak actually dominates the OH stretching spectral region. This observation is a result of the very small concentration of H_2O and the much larger (0.35 mole fraction) HOD concentration. The absolute intensity from the OH stretch of HOD is much weaker than the OH stretch of

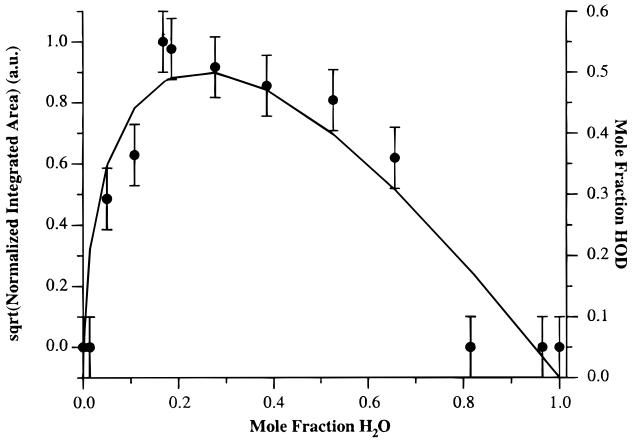

Figure 19. Plot of the square root of the normalized integrated area of the OH-S peak from HOD molecules, determined from fits to eqs 1 and 3, as a function of the mole fraction of H_2O. Solid line is a plot of the mole fraction of HOD as a function of the mole fraction of H_2O calculated using the equilibrium $H_2O + D_2O = 2HOD$ and $K = 4$.

H_2O. This decrease in intensity is a result of diminished hydrogen bonding and uncoupling of the OH stretching vibration from interfacial HOD molecules. The small peak present at approximately 3150 cm^{-1} in the low H_2O mole fraction spectra is most likely due to the tail of the O−D stretch from interfacial D_2O molecules.

We have fit the VSFS spectra for all the mole fraction solutions studied using two OH peaks, the OH-SS-S from H_2O and the OH-S from HOD, according to eqs 1 and 3. Using the fitted peaks, we have calculated the integrated area of the OH-S peak from interfacial HOD as a function of H_2O mole fraction. As mentioned earlier, the square root of the area of a peak in the VSFS spectrum is a good measure of the number of oscillators contributing to the SF signal; thus, in Figure 19 we plot the normalized square root of the peak area of the OH-S peak from interfacial HOD molecules as a function of the mole fraction of H_2O. In the same figure we plot the mole fraction of HOD as a function of the mole fraction of H_2O calculated assuming complete isotopic exchange and the equilibrium $H_2O + D_2O = 2HOD$ with $K = 4$. The agreement between the square root of the area of the peak at 3460 cm^{-1} and the mole fraction of HOD provides further evidence that the OH-S from HOD molecules is responsible for this peak. This work represents the first observation of the OH stretch from uncoupled HOD molecules at an CCl_4/water interface in the presence of a charged soluble surfactant and will be used in future studies to measure the properties of aqueous surfaces.

Conclusions and Future Directions

The structure and intermolecular hydrogen bonding of interfacial water molecules are essential to the description of many physical, chemical, and biological processes. This is no less true at aqueous surfaces than in bulk water or aqueous solutions. Our approach has been to employ vibrational sum frequency spectroscopy to probe interfacial water molecules by examining OH stretching modes sensitive to the structure and intermolecular hydrogen bonding. The studies presented here encompass a wide range of experimental conditions. Significant variations in the structure and intermolecular hydrogen bonding of interfacial water molecules are observed as experimental parameters are varied. Most notable is the fundamental difference in the structure and hydrogen bonding of water molecules at the neat air/water and CCl_4/water interfaces. In the classical description of the hydrophobic effect a nonpolar molecule is solvated by water through maximization of the intermolecular hydrogen bonding at the expense of entropy. Our observation that the VSF spectra from the neat air/water interface contains contributions from both OH peaks whereas the VSF spectra from the CCl_4/water interface contains only the OH-SS-S peak provides strong evidence for the classical description of the hydrophobic effect. Our future work in this area will focus on the structure and hydrogen bonding of surface water molecules adjacent to molecules in other hydrophobic phases of varying polarity. One might expect that more polar, yet still immiscible, molecules would have a smaller structure-inducing effect on the interfacial water molecules, resulting in a relative scale of hydrophobicity.

The function of common surfactants in such products as detergents and soaps arises from the micellization of oil or "dirt" particles by the surfactant molecules, thus increasing their solubility in water. Our studies of different common surfactants have focused on the effects that the headgroup has on the structure and intermolecular hydrogen bonding of interfacial water molecules. We find that neutral surfactants such as pentadecanoic acid produce little change in the structure and intermolecular hydrogen bonding of interfacial water molecules. In contrast to neutral surfactants, charged surfactants induce an alignment of the interfacial water molecules resulting from the electrostatic field that accompanies the surface charge. From the VSF spectra we are able to infer a relative orientation of the interfacial water molecules in the presence of cationic and anionic surfactants. We find that water molecules in the presence of cationic surfactants are oriented with their hydrogens pointed toward the bulk solution while water molecules in the presence of anionic surfactants are arranged with their oxygens pointed toward the bulk solution. Since both cationic and anionic surfactants are very effective as detergents and soaps, the orientation of water molecules around the micelle must play little role in the solubilization of dirt particles.

To further our understanding of water structure and bonding at a charged liquid surface, we have carried out detailed studies of the VSFS of water as the electrostatic properties of the double layer are varied. Of most importance in this area we find that at the air/water interface there is an increase in the extent of hydrogen bonding accompanying an increase in the surface potential or electrostatic field. Several experimental and theoretical studies conducted at the charged electrode/water interface have suggested that a strong electrostatic field can trigger a phase transition in the water molecules next to the charged surfaces.[54−56] The fact that we observe increased hydrogen bonding accompanying increased surface charge is in excellent agreement with the observations of water at the surface of a charged electrode. It is well-known that the surface tension of water decreases as surfactant is adsorbed to the surface, the decrease presumably a result of the surfactant molecules breaking up the strong interactions between water molecules. Our studies tell us that this disruption is accompanied by an increase in structuring or hydrogen bonding of water molecules in the double-layer region due to the electrostatic field created by the charged surfactant and counterion. It is important to reiterate that in these studies we find that the electrostatic field plays a dominant role in our observations, because of its strength in the presence of these surfactants as well as the larger volume of interfacial water being probed relative at the charged interface relative to an uncharged interface. Studies are currently in progress to characterize further the interaction and bonding of water with solutes and surfactants at these interfaces, as well as studies involving the

spectroscopy of headgroup moieties of surface active agents and studies of surface water in the presence of uncharged surfactants and structure-making and structure-breaking solutes and surfactants. Excursions into other spectral regions afforded by our now expanded tunability in the IR will play a significant role in these studies, allowing us to examine other OH and OD modes as well as additional vibrational modes of solutes and solvents.

Our temperature-dependent studies indicate that an increase in temperature at both interfaces in the presence of surfactant causes water molecules in the double-layer region to take on a broader distribution of energies. This is evidenced by the broadening of the OH stretching peaks for both the air/water and CCl_4/water interface. It is well-known that the surface tension of water decreases as the temperature increases. These observations are consistent with that picture.

Finally, the more specific nature of the structure of water molecules at the CCl_4/water interface has been examined through isotopic dilution experiments. This work represents the first application of the isotopic dilution technique, extensively used in the study of the structure of bulk liquid water and ice, to probe the structure of surface water molecules. Through these studies we find that the OH-SS-S peak behaves in a manner very similar to the OH peak observed from ice with regard to isotopic dilution and uncoupling of the OH stretching vibrations. This observation provides further evidence that the water molecules at the CCl_4/water interface are in an ice-like arrangement, resulting in the maximization of hydrogen bonding. From the isotopic dilution work we have also been able to monitor for the first time the OH stretching vibration from interfacial HOD molecules which has been shown to be extremely sensitive to the local environment of water molecules. We plan to continue with the isotopic dilution studies in the future by first extending it to the air/water interface followed by studies of the neat interfaces. It is hoped that HOD studies will provide us with a more fundamental picture of the structure of water surfaces that is inherently difficult due to the complex coupling of vibrational modes between water molecules in bulk media.

Acknowledgment. The authors would like to thankfully acknowledge the Office of Naval Research and the National Science Foundation (CHE-9725751) and the Petroleum Research Fund of the American Chemical Society for support of this work.

References and Notes

(1) Jones, M. N.; Chapman, D. *Micelles, Monolayers, and Biomembranes*; Wiley-Liss: New York, 1995.

(2) Richmond, G. L. *Anal. Chem.* **1997**, *69*, 636A.

(3) Messmer, M. C.; Conboy, J. C.; Richmond, G. L. *J. Am. Chem. Soc.* **1995**, *117*, 8039.

(4) Walker, R. A.; Conboy, J. C.; Richmond, G. L. *Langmuir* **1997**, *13*, 3070.

(5) Gragson, D. E.; Richmond, G. L. *J. Chem. Phys.* **1997**, *107*, 9687.

(6) Bell, G. R.; Bain, C. D.; Ward, R. N. *J. Chem. Soc., Faraday Trans.* **1996**, *92*, 515.

(7) Conboy, J. C.; Messmer, M. C.; Richmond, G. L. *J. Phys. Chem.* **1996**, *100*, 7617.

(8) Du, Q.; Freysz, E.; Shen, Y. R. *Science* **1994**, *264*, 826.

(9) Gragson, D. E.; McCarty, B. M.; Richmond, G. L. *J. Am. Chem. Soc.* **1997**, *119*, 6144.

(10) Pflumio, V.; Vallet, J. C.; Boeglin, A. J.; Villaeys, A. A.; Lavoine, J. P. *Phys. Rev. A: At., Mol., Opt. Phys.* **1995**, *51*, 3174.

(11) Shen, Y. R. *Surf. Sci.* **1994**, *300*, 551.

(12) Zhao, X.; Ong, S.; Eisenthal, K. B. *Chem. Phys. Lett.* **1993**, *202*, 513.

(13) Chattoraj, D. K.; Birdi, K. S. *Adsorption and the Gibbs Surface Excess*; Plenum Press: New York, 1984.

(14) Gragson, D. E.; Alavi, D. S.; Richmond, G. L. *Opt. Lett.* **1995**, *20*, 1991.

(15) Gragson, D. E.; McCarty, B. M.; Richmond, G. L.; Alavi, D. S. *J. Opt. Soc. Am. B* **1996**, *13*, 2075.

(16) Tajima, K. *Bull. Chem. Soc. Jpn.* **1970**, *43*, 3063.

(17) Tajima, K. *Bull. Chem. Soc. Jpn.* **1971**, *44*, 1767.

(18) Du, Q.; Superfine, R.; Freysz, E.; Shen, Y. R. *Phys. Rev. Lett.* **1993**, *70*, 2313.

(19) Gragson, D. E.; Richmond, G. L. *Langmuir* **1997**, *13*, 4804.

(20) Eisenberg, D.; Kauzmann, W. *The Structure and Properties of Water*; Oxford University Press: New York, 1969.

(21) Scherer, J. R.; Go, M. K.; Kint, S. *J. Phys. Chem.* **1974**, *78*, 1304.

(22) *Water: A Comprehensive Treatise*; Walrafen, G. E., Ed.; Plenum Press: New York, 1972; Vol. 1, p 151.

(23) Yalamanchili, M. R.; Atia, A. A.; Miller, J. D. *Langmuir* **1996**, *12*, 4176.

(24) Giguere, P. A. *J. Raman Spectrosc.* **1984**, *15*, 354.

(25) Whalley, E. *Can. J. Chem.* **1977**, *55*, 3429.

(26) Green, J. L.; Lacey, A. R.; Sceats, M. G. *Chem. Phys. Lett.* **1986**, *130*, 67.

(27) Gragson, D. E.; Richmond, G. L. *J. Phys. Chem. B* **1998**, *102*, 569.

(28) Tanford, C. *The Hydrophobic Effect*; Wiley-Interscience: New York, 1973.

(29) Michael, D.; Benjamin, I. *J. Phys. Chem.* **1995**, *99*, 1530.

(30) Benjamin, I. *Chem. Rev.* **1996**, *96*, 1449.

(31) Carpenter, I. L.; Hehre, W. J. *J. Phys. Chem.* **1990**, *94*, 531.

(32) Kovaleski, J. M.; Wirth, M. J. *J. Phys. Chem.* **1995**, *99*, 4091.

(33) Wirth, M. J.; Burbage, J. D. *J. Phys. Chem.* **1992**, *96*, 9022.

(34) Guyot-Sionnest, P.; Hunt, J. H.; Shen, Y. R. *Phys. Rev. Lett.* **1987**, *59*, 1597.

(35) Hunt, J. H.; Guyot-Sionnest, P.; Shen, Y. R. *Chem. Phys. Lett.* **1987**, *133*, 189.

(36) Gragson, D. E.; McCarty, B. M.; Richmond, G. L. *J. Phys. Chem.* **1996**, *100*, 14272.

(37) Ong, S.; Zhao, X.; Eisenthal, K. B. *Chem. Phys. Lett.* **1992**, *191*, 327.

(38) Toney, M. F.; Howard, J. N.; Richer, J.; Borges, G. L.; Gordon, J. G.; Melroy, O. R.; Wiesler, D. G.; Yee, D.; Sorensen, L. B. *Nature* **1994**, *368*, 444.

(39) Gordon, J. D.; Melroy, O. R.; Toney, M. F. *Electrochim. Acta* **1995**, *40*, 3.

(40) Gragson, D. E.; Richmond, G. L. *J. Am. Chem. Soc.* **1998**, *120*, 366.

(41) Ataka, K.-I.; Yotsuyanagi, T.; Osawa, M. *J. Phys. Chem.* **1996**, *100*, 10664.

(42) Habib, M. A.; Bockris, J. O. M. *Langmuir* **1986**, *2*, 388.

(43) Schweighofer, K. J.; Essmann, U.; Berkowitz, M. *J. Phys. Chem. B* **1997**, *101*, 3793.

(44) Xia, X.; Berkowitz, M. *Phys. Rev. Lett.* **1995**, *74*, 3193.

(45) Xia, X.; Perera, L.; Essmann, U.; Berkowitz, M. L. *Surf. Sci.* **1995**, *335*, 401.

(46) Schweighofer, K. J.; Xia, X.; Berkowitz, M. L. *Langmuir* **1996**, *12*, 3747.

(47) Wiafe-Akenten, J.; Bansil, R. *J. Chem. Phys.* **1983**, *78*, 7132.

(48) Wall, T. T.; Horning, D. F. *J. Chem. Phys.* **1965**, *43*, 2079.

(49) Devlin, J. P. *J. Chem. Phys.* **1989**, *90*, 1322.

(50) Savatinova, I.; Anachkova, E.; Nikolaeva, R. *Spectrosc. Lett.* **1986**, *19*, 167.

(51) Wojcik, M. J.; Buch, V.; Devlin, J. P. *J. Chem. Phys.* **1993**, *99*, 2332.

(52) Scherer, J. R.; Snyder, R. G. *J. Chem. Phys.* **1977**, *67*, 4794.

(53) Green, J. L.; Lacey, A. R.; Sceats, M. G. *J. Phys. Chem.* **1986**, *90*, 3958.

(54) Bendersky, V. A.; Brodsky, A. M.; Velichko, G. I.; Daikhin, L. I. *Sov. Electrochem.* **1987**, *23*, 435.

(55) Brodsky, A. M.; Daikhin, L. I. *Sov. Electrochem.* **1989**, *25*, 379.

(56) Gavish, M.; Wang, J. L.; Eisenstein, M.; Lahav, M.; Leiserowitz, L. *Science* **1992**, *256*, 815.